POLITECNICO DI TORINO
Repository ISTITUZIONALE

Analysis of laminated doubly-curved shells by alayerwise theory and radial basis functions collocation, accounting for through-the-thickness deformations

Original
Analysis of laminated doubly-curved shells by alayerwise theory and radial basis functions collocation, accounting for through-the-thickness deformations / Ferreira, A. J. M.; Roque, C. C.; Carrera, Erasmo; Cinefra, Maria. - In: COMPUTATIONAL MECHANICS. - ISSN 0178-7675. - 48:1(2011), pp. 13-25. [10.1007/s00466-011-0579-4]

Availability:
This version is available at: 11583/2381389 since:

Publisher:
Springer

Published
DOI:10.1007/s00466-011-0579-4

Terms of use:

This article is made available under terms and conditions as specified in the corresponding bibliographic description in the repository

Publisher copyright

(Article begins on next page)

19 April 2024

Analysis of laminated doubly-curved shells by a layerwise theory and radial basis functions collocation, accounting for through-the-thickness deformations

A. J. M. Ferreira · E. Carrera · M. Cinefra · C. M. C. Roque

Abstract In this paper, the static and free vibration analysis of laminated shells is performed by radial basis functions (RBFs) collocation, according to a layerwise deformation theory (LW). The present LW theory accounts for through-the-thickness deformation, by considering an Mindlin-like evolution of all displacements in each layer. The equations of motion and the boundary conditions are obtained by Carrera's unified formulation, and further interpolated by collocation with RBFs.

Keywords Bending · Modeling · Numerical methods

1 Introduction

In recent years, considerable attention has been paid to the development of appropriate two-dimensional shell theories that can accurately describe the response of multilayered anisotropic thick shells. In fact, thick shell component analysis and fatigue design require an accurate description of local stress fields to include highly accurate assessment of localized regions where damage is likely to take place. Examples of multilayered shell structures used in modern aerospace vehicles are laminated constructions made of anisotropic composite materials, sandwich panels, layered structures used as thermal protection, or intelligent structural system embedding piezolayers.

Classical displacement formulations start by assuming a linear or higher-order expansion for the displacement fields in the thickness direction. In-plane and transverse stresses are then computed by means of Hooke's law. According to this procedure, it is found that transverse stresses (both shear and normal components) are discontinuous at the interfaces of the multi-layer structure. To overcome these difficulties, these stresses are evaluated a posteriori in most applications by implementing a postprocessing procedure, e.g., through the thickness integration of the three-dimensional indefinite equation of equilibrium. But, this procedure cannot be implemented for most of the available models in the general case of asymmetric in-plane displacement fields (i.e., two different results could be obtained for the stress distributions by starting from the top or from the bottom shell surface).

In this scenario, the classical two-dimensional models, such as Koiter [1] and Naghdi [2] models, require some amendments to study multi-layered shell structures. Among these, the inclusion of continuity of displacements—*zigzag effects* (see Fig. 1)—at the interface between two adjacent layers is one of the amendments necessary. The role played by zigzag effects has been confirmed by many three-dimensional analysis of layered shells [3–8]. Exhaustive overviews on classical and refined models of multilayered structures have been reported in many published review articles. These include the papers by Grigolyuk and Kulikov [9], Kapania and Raciti [10], Kapania [11], Noor et al. [12–14] and Soldatos and Timarci [15]. Among the refined theories a convenient distinction can be made between models in which the number of the unknown variables is

A. J. M. Ferreira (✉)
Departamento de Engenharia Mecânica, Faculdade de Engenharia da Universidade do Porto, Rua Dr. Roberto Frias, 4200-465 Porto, Portugal
e-mail: ferreira@fe.up.pt

E. Carrera · M. Cinefra
Department of Aeronautics and Aerospace Engineering, Politecnico di Torino, Corso Duca degli Abruzzi, 24, 10129 Turin, Italy

C. M. C. Roque
INEGI, Faculdade de Engenharia da Universidade do Porto, Rua Dr. Roberto Frias, 4200-465 Porto, Portugal

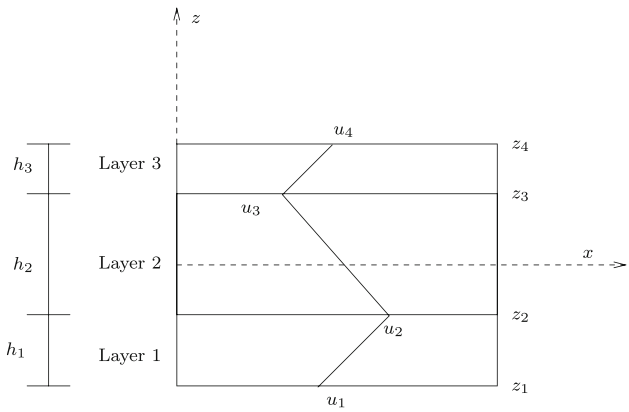

Fig. 1 Scheme of the layerwise assumptions for a three-layered laminate

independent or dependent on the number of the constitutive layers of the shell. Following Reddy [16], we assign the name ESLM (Equivalent Single Layer Models) to the first grouping while LWM (Layer Wise Model) is used to denote the others. Early [17–20] and more recent [21–26] LWMs have shown the superiority of layer-wise approaches over ESL approaches to predict accurately static and dynamic response of thick and very thick structures. On the other hand, LWMs are computationally expensive and the use of ESLMs is preferred in most practical applications.

In this paper, we propose to use the unified formulation (UF) by Carrera [27] to derive the equations of motion and boundary conditions to analyze laminated shells, according to a layerwise-based shear deformation theory that accounts for through-the-thickness deformations. The UF is a compact formulation that permits to analyze the bi-dimensional structures irrespective of the shear deformation theory being considered and it has been applied in several finite element analysis, either using the principle of virtual displacements (PVDs), or by using the Reissner's mixed variational theorem [28–31].

In the most general cases, the finite element method is used for the analysis of shell structures and some reviews on finite element shell formulations can be found in the work by Dennis and Palazotto [32], Merk [33], and Di and Ramm [34]. But, it is known that the phenomenon of numerical locking may arise from hidden constrains that are not well represented in the finite element approximation. The present paper, that performs the bending and free vibration analysis of laminated shells by collocation with radial basis functions (RBFs), avoids the locking phenomenon. A radial basis function RBF, $\phi(\|x - x_j\|)$ is a spline that depends on the Euclidian distance between distinct data centers $x_{j,j} = 1, 2, \ldots, N \in \mathbb{R}^n$, also called nodal or collocation points. We use the so-called unsymmetrical Kansa method, that was introduced by Kansa [35]. The use of RBF for the analysis of structures and materials has been previously studied by numerous authors [36–50]. The authors have recently applied the RBF collocation to the static deformations of composite beams and plates [51–53].

In this paper, it is investigated how the UF can be combined with RBFs to the analysis of thin and thick laminated shells, using the LW approach, allowing for through-the-thickness deformations. The quality of the present method in predicting static deformations and free vibrations of thin and thick laminated shells is compared and discussed with other methods in some numerical examples.

2 Unified formulation for the layerwise theory

The UF proposed by Carrera [54–57], also known as CUF, is a powerful framework for the analysis of beams, plates and shells. This formulation has been applied in several finite element analysis, either using the PVDs, or by using the Reissner's mixed variational theorem. The stiffness matrix components, the external force terms or the inertia terms can be obtained directly with this UF, irrespective of the shear deformation theory being considered.

In this section the Carrera's unified formulation is briefly reviewed. It is shown how to obtain the fundamental nuclei, which allows the derivation of the equations of motion and boundary conditions, in weak form for the finite element analysis; and in strong form for the present RBF collocation.

2.1 Shell geometry

Shells are bi-dimensional structures in which one dimension (in general the thickness in z direction) is negligible with respect to the other two in-plane dimensions. Geometry and the reference system are indicated in Fig. 3. The square of an infinitesimal linear segment in the layer, the associated infinitesimal area and volume are given by:

$$\begin{aligned} ds_k^2 &= H_\alpha^{k2}\, d\alpha^2 \;+\; H_\beta^{k2}\, d\beta^2 + H_z^{k2}\, dz^2, \\ d\Omega_k &= H_\alpha^k H_\beta^k\, d\alpha\, d\beta, \\ dV &= H_\alpha^k\, H_\beta^k\, H_z^k\, d\alpha\, d\beta\, dz, \end{aligned} \tag{1}$$

where the metric coefficients are:

$$H_\alpha^k = A^k(1+z/R_\alpha^k), \quad H_\beta^k = B^k(1+z/R_\beta^k), \quad H_z^k = 1. \tag{2}$$

k denotes the k-layer of the multilayered shell; R_α^k and R_β^k are the principal radii of curvature along the coordinates α and β respectively. A^k and B^k are the coefficients of the first fundamental form of Ω_k (Γ_k is the Ω_k boundary). In this work, the attention has been restricted to shells with constant radii of curvature (cylindrical, spherical, toroidal geometries) for which $A^k = B^k = 1$.

2.2 Governing equations and boundary conditions

Although one can use the UF for one-layer, isotropic shell, a multi-layered shell with N_l layers is considered. The PVDs for the pure-mechanical case reads:

$$\sum_{k=1}^{N_l} \int_{\Omega_k} \int_{A_k} \left\{ \delta \epsilon_{pG}^{k\ T} \sigma_{pC}^k + \delta \epsilon_{nG}^{k\ T} \sigma_{nC}^k \right\} d\Omega_k dz = \sum_{k=1}^{N_l} \delta L_e^k \tag{3}$$

where Ω_k and A_k are the integration domains in plane (α, β) and z direction, respectively. Here, k indicates the layer and T the transpose of a vector, and δL_e^k is the external work for the kth layer. G means geometrical relations and C constitutive equations.

The steps to obtain the governing equations are:

- Substitution of the geometrical relations (subscript G).
- Substitution of the appropriate constitutive equations (subscript C).
- Introduction of the unified formulation.

Stresses and strains are separated into in-plane and normal components, denoted respectively by the subscripts p and n. The mechanical strains in the kth layer can be related to the displacement field $\mathbf{u}^k = \{u_\alpha^k, u_\beta^k, u_z^k\}$ via the geometrical relations:

$$\begin{aligned} \epsilon_{pG}^k &= [\epsilon_{\alpha\alpha}^k, \epsilon_{\beta\beta}^k, \epsilon_{\alpha\beta}^k]^T = (\boldsymbol{D}_p^k + \boldsymbol{A}_p^k)\, \boldsymbol{u}^k, \\ \epsilon_{nG}^k &= [\epsilon_{\alpha z}^k, \epsilon_{\beta z}^k, \epsilon_{zz}^k]^T = (\boldsymbol{D}_{n\Omega}^k + \boldsymbol{D}_{nz}^k - \boldsymbol{A}_n^k)\, \boldsymbol{u}^k \end{aligned} \tag{4}$$

The explicit form of the introduced arrays follows:

$$\boldsymbol{D}_p^k = \begin{bmatrix} \frac{\partial_\alpha}{H_\alpha^k} & 0 & 0 \\ 0 & \frac{\partial_\beta}{H_\beta^k} & 0 \\ \frac{\partial_\beta}{H_\beta^k} & \frac{\partial_\alpha}{H_\alpha^k} & 0 \end{bmatrix}, \quad \boldsymbol{D}_{n\Omega}^k = \begin{bmatrix} 0 & 0 & \frac{\partial_\alpha}{H_\alpha^k} \\ 0 & 0 & \frac{\partial_\beta}{H_\beta^k} \\ 0 & 0 & 0 \end{bmatrix},$$

$$\boldsymbol{D}_{nz}^k = \begin{bmatrix} \partial_z & 0 & 0 \\ 0 & \partial_z & 0 \\ 0 & 0 & \partial_z \end{bmatrix}, \tag{5}$$

$$\boldsymbol{A}_p^k = \begin{bmatrix} 0 & 0 & \frac{1}{H_\alpha^k R_\alpha^k} \\ 0 & 0 & \frac{1}{H_\beta^k R_\beta^k} \\ 0 & 0 & 0 \end{bmatrix}, \quad \boldsymbol{A}_n^k = \begin{bmatrix} \frac{1}{H_\alpha^k R_\alpha^k} & 0 & 0 \\ 0 & \frac{1}{H_\beta^k R_\beta^k} & 0 \\ 0 & 0 & 0 \end{bmatrix}. \tag{6}$$

The 3D constitutive equations are given as:

$$\begin{aligned} \sigma_{pC}^k &= \mathbf{C}_{pp}^k\, \epsilon_{pG}^k + \mathbf{C}_{pn}^k\, \epsilon_{nG}^k \\ \sigma_{nC}^k &= \mathbf{C}_{np}^k\, \epsilon_{pG}^k + \mathbf{C}_{nn}^k\, \epsilon_{nG}^k \end{aligned} \tag{7}$$

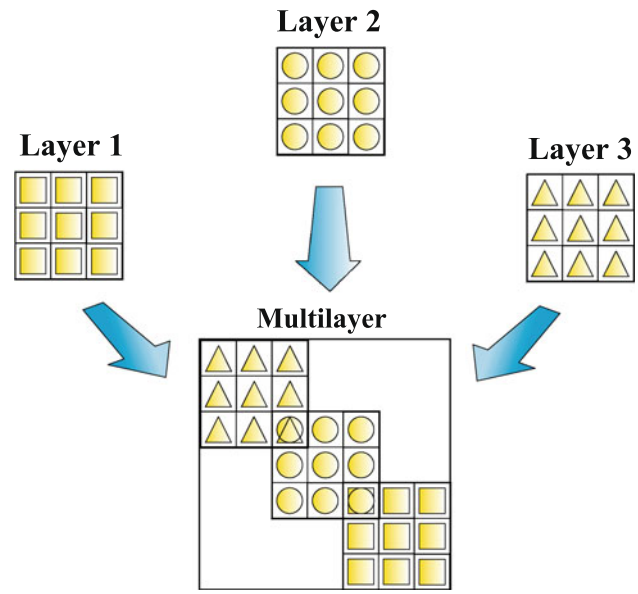

Fig. 2 Assembling procedure for LW approach

with

$$\mathbf{C}_{pp}^k = \begin{bmatrix} C_{11}^k & C_{12}^k & C_{16}^k \\ C_{12}^k & C_{22}^k & C_{26}^k \\ C_{16}^k & C_{26}^k & C_{66}^k \end{bmatrix} \quad \mathbf{C}_{pn}^k = \begin{bmatrix} 0 & 0 & C_{13}^k \\ 0 & 0 & C_{23}^k \\ 0 & 0 & C_{36}^k \end{bmatrix}$$

$$\mathbf{C}_{np}^k = \begin{bmatrix} 0 & 0 & 0 \\ 0 & 0 & 0 \\ C_{13}^k & C_{23}^k & C_{36}^k \end{bmatrix} \quad \mathbf{C}_{nn}^k = \begin{bmatrix} C_{55}^k & C_{45}^k & 0 \\ C_{45}^k & C_{44}^k & 0 \\ 0 & 0 & C_{33}^k \end{bmatrix} \tag{8}$$

In case of layer wise (LW) models, each layer k of the given multi-layered structure is separately considered. According to the CUF, the three displacement components u_α, u_β and u_z and their relative variations can be modelled as:

$$\begin{aligned} (u_\alpha^k, u_\beta^k, u_z^k) &= F_\tau^k\ (u_{\alpha\tau}^k, u_{\beta\tau}^k, u_{z\tau}^k) \\ (\delta u_\alpha^k, \delta u_\beta^k, \delta u_z^k) &= F_s^k\ (\delta u_{\alpha s}^k, \delta u_{\beta s}^k, \delta u_{zs}^k) \end{aligned} \tag{9}$$

In the present formulation, we choose:

$$F_\tau^k = \left[\frac{1 - 2/h_k \left(z - \frac{1}{2}(z_k + z_{k+1})\right)}{2} \times \frac{1 + 2/h_k \left(z - \frac{1}{2}(z_k + z_{k+1})\right)}{2} \right]$$

for displacements u, v, w. Note that z_k, z_{k+1} correspond to the bottom and top z-coordinates for each layer k. We then obtain all terms of the equations of motion by integrating through the thickness direction. In Fig. 2 it is shown the assembling procedure on layer k for the LW approach.

It is interesting to note that under this combination of the UF and RBF collocation, the collocation code depends only on the choice of F_t, F_s, in order to solve this type of problems.

We designed a MATLAB code that just by changing F_t, F_s can analyse static deformations and free vibrations for any type of C^0 shear deformation theory.

Substituting the geometrical relations, the constitutive equations and the UF into the variational statement PVD, for the kth layer, one has:

$$\sum_{k=1}^{N_l}\left\{\int_{\Omega_k}\int_{A_k}\{((\boldsymbol{D}_p+\boldsymbol{A}_p)\delta\boldsymbol{u}^k)^T(\boldsymbol{C}^k_{pp}(\boldsymbol{D}_p+\boldsymbol{A}_p)\boldsymbol{u}^k \right.$$
$$+\boldsymbol{C}^k_{pn}(\boldsymbol{D}_{n\Omega}+\boldsymbol{D}_{nz}-\boldsymbol{A}_n)\boldsymbol{u}^k)$$
$$+((\boldsymbol{D}_{n\Omega}+\boldsymbol{D}_{nz}-\boldsymbol{A}_n)\delta\boldsymbol{u}^k)^T(\boldsymbol{C}^k_{np}(\boldsymbol{D}_p+\boldsymbol{A}_p)\boldsymbol{u}^k$$
$$\left.+\boldsymbol{C}^k_{nn}(\boldsymbol{D}_{n\Omega}+\boldsymbol{D}_{nz}-\boldsymbol{A}_n)\boldsymbol{u}^k)\}d\Omega_k dz_k\right\}$$
$$=\sum_{k=1}^{N_l}\delta L^k_e \tag{10}$$

At this point, the formula of integration by parts is applied:

$$\int_{\Omega_k}\left((\mathbf{D}_\Omega)\delta\mathbf{a}^k\right)^T\mathbf{a}^k d\Omega_k=-\int_{\Omega_k}\delta\mathbf{a}^{kT}\left((\mathbf{D}^T_\Omega)\mathbf{a}^k\right)d\Omega_k$$
$$+\int_{\Gamma_k}\delta\mathbf{a}^{kT}\left((\mathbf{I}_\Omega)\mathbf{a}^k\right)d\Gamma_k \tag{11}$$

where $\mathbf{I}_\Omega$ matrix is obtained applying the *Gradient theorem*:

$$\int_\Omega\frac{\partial\psi}{\partial x_i}d\upsilon=\oint_\Gamma n_i\psi ds \tag{12}$$

being n_i the components of the normal $\widehat{n}$ to the boundary along the direction i. After integration by parts and the substitution of CUF, the governing equations and boundary conditions for the shell in the mechanical case are obtained:

$$\sum_{k=1}^{N_l}\left\{\int_{\Omega_k}\int_{A_k}\left\{\delta\boldsymbol{u}^{kT}_s\left[(-\boldsymbol{D}_p+\boldsymbol{A}_p)^T F_s(\boldsymbol{C}^k_{pp}(\boldsymbol{D}_p+\boldsymbol{A}_p)F_\tau\boldsymbol{u}^k_\tau\right.\right.\right.$$
$$\left.+\boldsymbol{C}^k_{pn}(\boldsymbol{D}_{n\Omega}+\boldsymbol{D}_{nz}-\boldsymbol{A}_n)F_\tau\boldsymbol{u}^k_\tau)\right]$$
$$+\delta\boldsymbol{u}^{kT}_s\left[(-\boldsymbol{D}_{n\Omega}+\boldsymbol{D}_{nz}-\boldsymbol{A}_n)^T F_s(\boldsymbol{C}^k_{np}(\boldsymbol{D}_p+\boldsymbol{A}_p)F_\tau\boldsymbol{u}^k_\tau\right.$$
$$\left.\left.\left.+\boldsymbol{C}^k_{nn}(\boldsymbol{D}_{n\Omega}+\boldsymbol{D}_{nz}-\boldsymbol{A}_n)F_\tau\boldsymbol{u}^k_\tau)\right]\right\}d\Omega_k dz_k\right\}$$
$$+\sum_{k=1}^{N_l}\left\{\int_{\Gamma_k}\int_{A_k}\left\{\delta\boldsymbol{u}^{kT}_s\left[\boldsymbol{I}^T_p F_s(\boldsymbol{C}^k_{pp}(\boldsymbol{D}_p+\boldsymbol{A}_p)F_\tau\boldsymbol{u}^k_\tau\right.\right.\right.$$
$$\left.+\boldsymbol{C}^k_{pn}(\boldsymbol{D}_{n\Omega}+\boldsymbol{D}_{nz}-\boldsymbol{A}_n)F_\tau\boldsymbol{u}^k_\tau)\right]$$
$$+\delta\boldsymbol{u}^{kT}_s\left[\boldsymbol{I}^T_{np}F_s\left(\boldsymbol{C}^k_{np}(\boldsymbol{D}_p-\boldsymbol{A}_p)F_\tau\boldsymbol{u}^k_\tau\right.\right.$$
$$\left.\left.\left.\left.+\boldsymbol{C}^k_{nn}(\boldsymbol{D}_{n\Omega}+\boldsymbol{D}_{nz}-\boldsymbol{A}_n)F_\tau\boldsymbol{u}^k_\tau\right)\right]\right\}d\Gamma_k dz_k\right\}$$
$$=\sum_{k=1}^{N_l}\left\{\int_{\Omega_k}\delta\boldsymbol{u}^{kT}_s F_s\boldsymbol{p}^k_u\right\}. \tag{13}$$

where $\mathbf{I}^k_p$ and $\mathbf{I}^k_{np}$ depend on the boundary geometry:

$$\mathbf{I}_p=\begin{bmatrix}\frac{n_\alpha}{H_\alpha} & 0 & 0\\ 0 & \frac{n_\beta}{H_\beta} & 0\\ \frac{n_\beta}{H_\beta} & \frac{n_\alpha}{H_\alpha} & 0\end{bmatrix};\ \mathbf{I}_{np}=\begin{bmatrix}0 & 0 & \frac{n_\alpha}{H_\alpha}\\ 0 & 0 & \frac{n_\beta}{H_\beta}\\ 0 & 0 & 0\end{bmatrix}. \tag{14}$$

The normal to the boundary of domain Ω is:

$$\widehat{\boldsymbol{n}}=\begin{bmatrix}n_\alpha\\ n_\beta\end{bmatrix}=\begin{bmatrix}cos(\varphi_\alpha)\\ cos(\varphi_\beta)\end{bmatrix} \tag{15}$$

where φ_α and φ_β are the angles between the normal $\widehat{n}$ and the direction α and β respectively.

The governing equations for a multi-layered shell subjected to mechanical loadings are:

$$\delta\mathbf{u}^{kT}_s:\mathbf{K}^{k\tau s}_{uu}\,\mathbf{u}^k_\tau\ =\ \mathbf{P}^k_{u\tau} \tag{16}$$

where the fundamental nucleus $\mathbf{K}^{k\tau s}_{uu}$ is obtained as:

$$\boldsymbol{K}^{k\tau s}_{uu}=\int_{A_k}\left[[-\boldsymbol{D}_p+\boldsymbol{A}_p]^T\,\boldsymbol{C}^k_{pp}[\boldsymbol{D}_p+\boldsymbol{A}_p]\right.$$
$$+[-\boldsymbol{D}_p+\boldsymbol{A}_p]^T\,\boldsymbol{C}^k_{pn}[\boldsymbol{D}_{n\Omega}+\boldsymbol{D}_{nz}-\boldsymbol{A}_n]$$
$$+[-\boldsymbol{D}_{n\Omega}+\boldsymbol{D}_{nz}-\boldsymbol{A}_n]^T\,\boldsymbol{C}^k_{np}[\boldsymbol{D}_p+\boldsymbol{A}_p]$$
$$\left.+[-\boldsymbol{D}_{n\Omega}+\boldsymbol{D}_{nz}-\boldsymbol{A}_n]^T\,\boldsymbol{C}^k_{nn}[\boldsymbol{D}_{n\Omega}+\boldsymbol{D}_{nz}-\boldsymbol{A}_n]\right]$$
$$\times F_\tau F_s H^k_\alpha H^k_\beta\,dz. \tag{17}$$

and the corresponding Neumann-type boundary conditions on Γ_k are:

$$\boldsymbol{\Pi}^{k\tau s}_d\,\mathbf{u}^k_\tau\ =\ \boldsymbol{\Pi}^{k\tau s}_d\,\bar{\mathbf{u}}^k_\tau, \tag{18}$$

where:

$$\boldsymbol{\Pi}^{k\tau s}_d=\int_{A_k}\left[\boldsymbol{I}^T_p\,\boldsymbol{C}^k_{pp}[\boldsymbol{D}_p+\boldsymbol{A}_p]\right.$$
$$+\boldsymbol{I}^T_p\,\boldsymbol{C}^k_{pn}[\boldsymbol{D}_{n\Omega}+\boldsymbol{D}_{nz}-\boldsymbol{A}_n]$$
$$+\boldsymbol{I}^T_{np}\boldsymbol{C}^k_{np}[\boldsymbol{D}_p+\boldsymbol{A}_p]$$
$$\left.+\boldsymbol{I}^T_{np}\,\boldsymbol{C}^k_{nn}[\boldsymbol{D}_{n\Omega}+\boldsymbol{D}_{nz}-\boldsymbol{A}_n]\right]F_\tau F_s H^k_\alpha H^k_\beta\,dz. \tag{19}$$

and $\mathbf{P}^k_{u\tau}$ are variationally consistent loads with applied pressure.

2.3 Fundamental nuclei

The following integrals are introduced to perform the explicit form of fundamental nuclei:

$$
\begin{aligned}
&(J^{k\tau s}, J_{\alpha}^{k\tau s}, J_{\beta}^{k\tau s}, J_{\frac{\alpha}{\beta}}^{k\tau s}, J_{\frac{\beta}{\alpha}}^{k\tau s}, J_{\alpha\beta}^{k\tau s}) \\
&\quad = \int_{A_k} F_\tau F_s \left(1, H_\alpha, H_\beta, \frac{H_\alpha}{H_\beta}, \frac{H_\beta}{H_\alpha}, H_\alpha H_\beta\right) dz \\
&\left(J^{k\tau_z s}, J_{\alpha}^{k\tau_z s}, J_{\beta}^{k\tau_z s}, J_{\frac{\alpha}{\beta}}^{k\tau_z s}, J_{\frac{\beta}{\alpha}}^{k\tau_z s}, J_{\alpha\beta}^{k\tau_z s}\right) \\
&\quad = \int_{A_k} \frac{\partial F_\tau}{\partial z} F_s \left(1, H_\alpha, H_\beta, \frac{H_\alpha}{H_\beta}, \frac{H_\beta}{H_\alpha}, H_\alpha H_\beta\right) dz \\
&\left(J^{k\tau s_z}, J_{\alpha}^{k\tau s_z}, J_{\beta}^{k\tau s_z}, J_{\frac{\alpha}{\beta}}^{k\tau s_z}, J_{\frac{\beta}{\alpha}}^{k\tau s_z}, J_{\alpha\beta}^{k\tau s_z}\right) \\
&\quad = \int_{A_k} F_\tau \frac{\partial F_s}{\partial z} \left(1, H_\alpha, H_\beta, \frac{H_\alpha}{H_\beta}, \frac{H_\beta}{H_\alpha}, H_\alpha H_\beta\right) dz \\
&\left(J^{k\tau_z s_z}, J_{\alpha}^{k\tau_z s_z}, J_{\beta}^{k\tau_z s_z}, J_{\frac{\alpha}{\beta}}^{k\tau_z s_z}, J_{\frac{\beta}{\alpha}}^{k\tau_z s_z}, J_{\alpha\beta}^{k\tau_z s_z}\right) \\
&\quad = \int_{A_k} \frac{\partial F_\tau}{\partial z} \frac{\partial F_s}{\partial z} \left(1, H_\alpha, H_\beta, \frac{H_\alpha}{H_\beta}, \frac{H_\beta}{H_\alpha}, H_\alpha H_\beta\right) dz
\end{aligned} \tag{20}
$$

The fundamental nucleo $\mathbf{K}_{uu}^{k\tau s}$ is reported for doubly curved shells (radii of curvature in both α and β directions, see Fig. 3):

$$
\begin{aligned}
\left(\mathbf{K}_{uu}^{\tau sk}\right)_{11} = & -C_{11}^k J_{\beta/\alpha}^{k\tau s} \partial_\alpha^s \partial_\alpha^\tau - C_{16}^k J^{k\tau s} \partial_\alpha^\tau \partial_\beta^s - C_{16}^k J^{k\tau s} \partial_\alpha^s \partial_\beta^\tau \\
& - C_{66}^k J_{\alpha/\beta}^{k\tau s} \partial_\beta^s \partial_\beta^\tau \\
& + C_{55}^k \left(J_{\alpha\beta}^{k\tau_z s_z} - \frac{1}{R_{\alpha_k}} J_{\beta}^{k\tau_z s} - \frac{1}{R_{\alpha_k}} J_{\beta}^{k\tau s_z} + \frac{1}{R_{\alpha_k}^2} J_{\beta/\alpha}^{k\tau s} \right) \\
\left(\mathbf{K}_{uu}^{\tau sk}\right)_{12} = & -C_{12}^k J^{k\tau s} \partial_\alpha^\tau \partial_\beta^s - C_{16}^k J_{\beta/\alpha}^{k\tau s} \partial_\alpha^s \partial_\alpha^\tau - C_{26}^k J_{\alpha/\beta}^{k\tau s} \partial_\beta^s \partial_\beta^\tau \\
& - C_{66}^k J^{k\tau s} \partial_\alpha^s \partial_\beta^\tau \\
& + C_{45}^k \left(J_{\alpha\beta}^{k\tau_z s_z} - \frac{1}{R_{\beta_k}} J_{\alpha}^{k\tau_z s} - \frac{1}{R_{\alpha_k}} J_{\beta}^{k\tau s_z} \right. \\
& \left. + \frac{1}{R_{\alpha_k}} \frac{1}{R_{\beta_k}} J^{k\tau s} \right) \\
\left(\mathbf{K}_{uu}^{\tau sk}\right)_{13} = & -C_{11}^k \frac{1}{R_{\alpha_k}} J_{\beta/\alpha}^{k\tau s} \partial_\alpha^\tau - C_{12}^k \frac{1}{R_{\beta_k}} J^{k\tau s} \partial_\alpha^\tau \\
& - C_{13}^k J_{\beta}^{k\tau s_z} \partial_\alpha^\tau \\
& - C_{16}^k \frac{1}{R_{\alpha_k}} J^{k\tau s} \partial_\beta^\tau - C_{26}^k \frac{1}{R_{\beta_k}} J_{\alpha/\beta}^{k\tau s} \partial_\beta^\tau \\
& - C_{36}^k J_{\alpha}^{k\tau s_z} \partial_\beta^\tau \\
& + C_{45}^k \left(J_{\alpha}^{k\tau_z s} \partial_\beta^s - \frac{1}{R_{\alpha_k}} J^{k\tau s} \partial_\beta^s \right) \\
& + C_{55}^k \left(J_{\beta}^{k\tau_z s} \partial_\alpha^s - \frac{1}{R_{\alpha_k}} J_{\beta/\alpha}^{k\tau s} \partial_\alpha^s \right)
\end{aligned}
$$

$$
\begin{aligned}
\left(\mathbf{K}_{uu}^{\tau sk}\right)_{21} = & -C_{12}^k J^{k\tau s} \partial_\alpha^s \partial_\beta^\tau - C_{16}^k J_{\beta/\alpha}^{k\tau s} \partial_\alpha^s \partial_\alpha^\tau - C_{26}^k J_{\alpha/\beta}^{k\tau s} \partial_\beta^s \partial_\beta^\tau \\
& - C_{66}^k J^{k\tau s} \partial_\alpha^\tau \partial_\beta^s \\
& + C_{45}^k \left(J_{\alpha\beta}^{k\tau_z s_z} - \frac{1}{R_{\beta_k}} J_{\alpha}^{k\tau s_z} - \frac{1}{R_{\alpha_k}} J_{\beta}^{k\tau_z s} \right. \\
& \left. + \frac{1}{R_{\alpha_k}} \frac{1}{R_{\beta_k}} J^{k\tau s} \right) \\
\left(\mathbf{K}_{uu}^{\tau sk}\right)_{22} = & -C_{22}^k J_{\alpha/\beta}^{k\tau s} \partial_\beta^s \partial_\beta^\tau - C_{26}^k J^{k\tau s} \partial_\alpha^s \partial_\beta^\tau - C_{26}^k J^{k\tau s} \partial_\alpha^\tau \partial_\beta^s \\
& - C_{66}^k J_{\beta/\alpha}^{k\tau s} \partial_\alpha^s \partial_\alpha^\tau \\
& + C_{44}^k \left(J_{\alpha\beta}^{k\tau_z s_z} - \frac{1}{R_{\beta_k}} J_{\alpha}^{k\tau_z s} - \frac{1}{R_{\beta_k}} J_{\alpha}^{k\tau s_z} + \frac{1}{R_{\beta_k}^2} J_{\alpha/\beta}^{k\tau s} \right) \\
\left(\mathbf{K}_{uu}^{\tau sk}\right)_{23} = & -C_{12}^k \frac{1}{R_{\alpha_k}} J^{k\tau s} \partial_\beta^\tau - C_{22}^k \frac{1}{R_{\beta_k}} J_{\alpha/\beta}^{k\tau s} \partial_\beta^\tau - C_{23}^k J_{\alpha}^{k\tau s_z} \partial_\beta^\tau \\
& - C_{16}^k \frac{1}{R_{\alpha_k}} J_{\beta/\alpha}^{k\tau s} \partial_\alpha^\tau - C_{26}^k \frac{1}{R_{\beta_k}} J^{k\tau s} \partial_\alpha^\tau \\
& - C_{36}^k J_{\beta}^{k\tau s_z} \partial_\alpha^\tau \\
& + C_{45}^k \left(J_{\beta}^{k\tau_z s} \partial_\alpha^s - \frac{1}{R_{\beta_k}} J^{k\tau s} \partial_\alpha^s \right) \\
& + C_{44}^k \left(J_{\alpha}^{k\tau_z s} \partial_\beta^s - \frac{1}{R_{\beta_k}} J_{\alpha/\beta}^{k\tau s} \partial_\beta^s \right)
\end{aligned}
$$

$$
\begin{aligned}
\left(\mathbf{K}_{uu}^{\tau sk}\right)_{31} = & C_{11}^k \frac{1}{R_{\alpha_k}} J_{\beta/\alpha}^{k\tau s} \partial_\alpha^s + C_{12}^k \frac{1}{R_{\beta_k}} J^{k\tau s} \partial_\alpha^s + C_{13}^k J_{\beta}^{k\tau_z s} \partial_\alpha^s \\
& + C_{16}^k \frac{1}{R_{\alpha_k}} J^{k\tau s} \partial_\beta^s + C_{26}^k \frac{1}{R_{\beta_k}} J_{\alpha/\beta}^{k\tau s} \partial_\beta^s \\
& + C_{36}^k J_{\alpha}^{k\tau_z s} \partial_\beta^s \\
& - C_{45}^k \left(J_{\alpha}^{k\tau s_z} \partial_\beta^\tau - \frac{1}{R_{\alpha_k}} J^{k\tau s} \partial_\beta^\tau \right) \\
& - C_{55}^k \left(J_{\beta}^{k\tau s_z} \partial_\alpha^\tau - \frac{1}{R_{\alpha_k}} J_{\beta/\alpha}^{k\tau s} \partial_\alpha^\tau \right) \\
\left(\mathbf{K}_{uu}^{\tau sk}\right)_{32} = & C_{12}^k \frac{1}{R_{\alpha_k}} J^{k\tau s} \partial_\beta^s + C_{22}^k \frac{1}{R_{\beta_k}} J_{\alpha/\beta}^{k\tau s} \partial_\beta^s + C_{23}^k J_{\alpha}^{k\tau_z s} \partial_\beta^s \\
& + C_{16}^k \frac{1}{R_{\alpha_k}} J_{\beta/\alpha}^{k\tau s} \partial_\alpha^s + C_{26}^k \frac{1}{R_{\beta_k}} J^{k\tau s} \partial_\alpha^s \\
& + C_{36}^k J_{\beta}^{k\tau_z s} \partial_\alpha^s \\
& - C_{45}^k \left(J_{\beta}^{k\tau s_z} \partial_\alpha^\tau - \frac{1}{R_{\beta_k}} J^{k\tau s} \partial_\alpha^\tau \right) \\
& - C_{44}^k \left(J_{\alpha}^{k\tau s_z} \partial_\beta^\tau - \frac{1}{R_{\beta_k}} J_{\alpha/\beta}^{k\tau s} \partial_\beta^\tau \right) \\
\left(\mathbf{K}_{uu}^{\tau sk}\right)_{33} = & C_{11}^k \frac{1}{R_{\alpha_k}^2} J_{\beta/\alpha}^{k\tau s} + C_{22}^k \frac{1}{R_{\beta_k}^2} J_{\alpha/\beta}^{k\tau s} + C_{33}^k J_{\alpha\beta}^{k\tau_z s_z} \\
& + 2C_{12}^k \frac{1}{R_{\alpha_k}} \frac{1}{R_{\beta_k}} J^{k\tau s} + C_{13}^k \frac{1}{R_{\alpha_k}} \left(J_{\beta}^{k\tau_z s} + J_{\beta}^{k\tau s_z} \right) \\
& + C_{23}^k \frac{1}{R_{\beta_k}} \left(J_{\alpha}^{k\tau_z s} + J_{\alpha}^{k\tau s_z} \right)
\end{aligned}
$$

$$-C_{44}^k J_{\alpha/\beta}^{k\tau s}\partial_\beta^s\partial_\beta^\tau - C_{55}^k J_{\beta/\alpha}^{k\tau s}\partial_\alpha^s\partial_\alpha^\tau$$
$$-C_{45}^k J^{k\tau s}\partial_\alpha^s\partial_\beta^\tau - C_{45}^k J^{k\tau s}\partial_\alpha^\tau\partial_\beta^s \tag{21}$$

The application of boundary conditions makes use of the fundamental nucleo $\mathbf{\Pi}_d$ in the form:

$$\begin{aligned}
\left(\mathbf{\Pi}_{uu}^{\tau sk}\right)_{11} &= n_\alpha C_{11}^k J_{\beta/\alpha}^{k\tau s}\partial_\alpha^s + n_\beta C_{66}^k J_{\alpha/\beta}^{k\tau s}\partial_\beta^s \\
&\quad + n_\beta C_{16}^k J^{k\tau s}\partial_\alpha^s + n_\alpha C_{16}^k J^{k\tau s}\partial_\beta^s \\
\left(\mathbf{\Pi}_{uu}^{\tau sk}\right)_{12} &= n_\alpha C_{16}^k J_{\beta/\alpha}^{k\tau s}\partial_\alpha^s + n_\beta C_{26}^k J_{\alpha/\beta}^{k\tau s}\partial_\beta^s \\
&\quad + n_\alpha C_{12}^k J^{k\tau s}\partial_\beta^s + n_\beta C_{66}^k J^{k\tau s}\partial_\alpha^s \\
\left(\mathbf{\Pi}_{uu}^{\tau sk}\right)_{13} &= n_\alpha \frac{1}{R_{\alpha k}} C_{11}^k J_{\beta/\alpha}^{k\tau s} + n_\alpha \frac{1}{R_{\beta k}} C_{12}^k J^{k\tau s} \\
&\quad + n_\alpha C_{13}^k J_\beta^{k\tau s_z} + n_\beta \frac{1}{R_{\alpha k}} C_{16}^k J^{k\tau s} \\
&\quad + n_\beta \frac{1}{R_{\beta k}} C_{26}^k J_{\alpha/\beta}^{k\tau s} + n_\beta C_{36}^k J_\alpha^{k\tau s_z} \\
\left(\mathbf{\Pi}_{uu}^{\tau sk}\right)_{21} &= n_\alpha C_{16}^k J_{\beta/\alpha}^{k\tau s}\partial_\alpha^s + n_\beta C_{26}^k J_{\alpha/\beta}^{k\tau s}\partial_\beta^s \\
&\quad + n_\beta C_{12}^k J^{k\tau s}\partial_\alpha^s + n_\alpha C_{66}^k J^{k\tau s}\partial_\beta^s \\
\left(\mathbf{\Pi}_{uu}^{\tau sk}\right)_{22} &= n_\alpha C_{66}^k J_{\beta/\alpha}^{k\tau s}\partial_\alpha^s + n_\beta C_{22}^k J_{\alpha/\beta}^{k\tau s}\partial_\beta^s \\
&\quad + n_\beta C_{26}^k J^{k\tau s}\partial_\alpha^s + n_\alpha C_{26}^k J^{k\tau s}\partial_\beta^s \\
\left(\mathbf{\Pi}_{uu}^{\tau sk}\right)_{23} &= n_\alpha \frac{1}{R_{\alpha k}} C_{16}^k J_{\beta/\alpha}^{k\tau s} + n_\alpha \frac{1}{R_{\beta k}} C_{26}^k J^{k\tau s} \\
&\quad + n_\alpha C_{36}^k J_\beta^{k\tau s_z} + n_\beta \frac{1}{R_{\alpha k}} C_{12}^k J^{k\tau s} \\
&\quad + n_\beta \frac{1}{R_{\beta k}} C_{22}^k J_{\alpha/\beta}^{k\tau s} + n_\beta C_{23}^k J_\alpha^{k\tau s_z} \\
\left(\mathbf{\Pi}_{uu}^{\tau sk}\right)_{31} &= -n_\alpha \frac{1}{R_{\alpha k}} C_{55}^k J_{\beta/\alpha}^{k\tau s} + n_\alpha C_{55}^k J_\beta^{k\tau s_z} \\
&\quad - n_\beta \frac{1}{R_{\alpha k}} C_{45}^k J^{k\tau s} + n_\beta C_{45}^k J_\alpha^{k\tau s_z} \\
\left(\mathbf{\Pi}_{uu}^{\tau sk}\right)_{32} &= -n_\alpha \frac{1}{R_{\beta k}} C_{45}^k J^{k\tau s} + n_\alpha C_{45}^k J_\beta^{k\tau s_z} \\
&\quad - n_\beta \frac{1}{R_{\beta k}} C_{44}^k J_{\alpha/\beta}^{k\tau s} + n_\beta C_{44}^k J_\alpha^{k\tau s_z} \\
\left(\mathbf{\Pi}_{uu}^{\tau sk}\right)_{33} &= n_\alpha C_{55}^k J_{\beta/\alpha}^{k\tau s}\partial_\alpha^s + n_\beta C_{44}^k J_{\alpha/\beta}^{k\tau s}\partial_\beta^s \\
&\quad + n_\beta C_{45}^k J^{k\tau s}\partial_\alpha^s + n_\alpha C_{45}^k J^{k\tau s}\partial_\beta^s
\end{aligned} \tag{22}$$

One can note that all the equations written for the shell degenerate in those for the plate when $\frac{1}{R_{\alpha k}} = \frac{1}{R_{\beta k}} = 0$. In practice we set the radii of curvature to 10^9.

2.4 Dynamic governing equations

The PVD for the dynamic case is expressed as:

$$\begin{aligned}
&\sum_{k=1}^{N_l} \int_{\Omega_k}\int_{A_k} \left\{ \delta\epsilon_{pG}^{k\,T}\sigma_{pC}^k + \delta\epsilon_{nG}^{k\,T}\sigma_{nC}^k \right\} d\Omega_k dz \\
&\quad = \sum_{k=1}^{N_l} \int_{\Omega_k}\int_{A_k} \rho^k \delta\mathbf{u}^{kT}\ddot{\mathbf{u}}^k d\Omega_k dz + \sum_{k=1}^{N_l} \delta L_e^k
\end{aligned} \tag{23}$$

where ρ^k is the mass density of the k-th layer and double dots denote acceleration.

By substituting the geometrical relations, the constitutive equations and the UF, we obtain the following governing equations:

$$\delta\mathbf{u}_s^{k\,T} \;:\; \mathbf{K}_{uu}^{k\tau s}\,\mathbf{u}_\tau^k = \mathbf{M}^{k\tau s}\ddot{\mathbf{u}}_\tau^k + \mathbf{P}_{u\tau}^k \tag{24}$$

In the case of free vibrations one has:

$$\delta\mathbf{u}_s^{k\,T} \;:\; \mathbf{K}_{uu}^{k\tau s}\,\mathbf{u}_\tau^k = \mathbf{M}^{k\tau s}\ddot{\mathbf{u}}_\tau^k \tag{25}$$

where $\mathbf{M}^{k\tau s}$ is the fundamental nucleus for the inertial term. The explicit form of that is:

$$\begin{aligned}
\mathbf{M}_{11}^{k\tau s} &= \rho^k J_{\alpha\beta}^{k\tau s} \\
\mathbf{M}_{12}^{k\tau s} &= 0 \\
\mathbf{M}_{13}^{k\tau s} &= 0 \\
\mathbf{M}_{21}^{k\tau s} &= 0 \\
\mathbf{M}_{22}^{k\tau s} &= \rho^k J_{\alpha\beta}^{k\tau s} \\
\mathbf{M}_{23}^{k\tau s} &= 0 \\
\mathbf{M}_{31}^{k\tau s} &= 0 \\
\mathbf{M}_{32}^{k\tau s} &= 0 \\
\mathbf{M}_{33}^{k\tau s} &= \rho^k J_{\alpha\beta}^{k\tau s}
\end{aligned} \tag{26}$$

where the meaning of the integral $J_{\alpha\beta}^{k\tau s}$ has been illustrated in Eq. (20). The geometrical and mechanical boundary conditions are the same of the static case. When we consider the static case, the mass terms are neglected.

3 The radial basis function method

3.1 The static problem

Radial basis functions (RBF) approximations are mesh-free numerical schemes that can exploit accurate representations of the boundary, are easy to implement and can be spectrally accurate. In this section the formulation of a global unsymmetrical collocation RBF-based method to compute elliptic operators is presented.

Consider a linear elliptic partial differential operator L and a bounded region Ω in $\mathbb{R}^n$ with some boundary $\partial\Omega$. In the

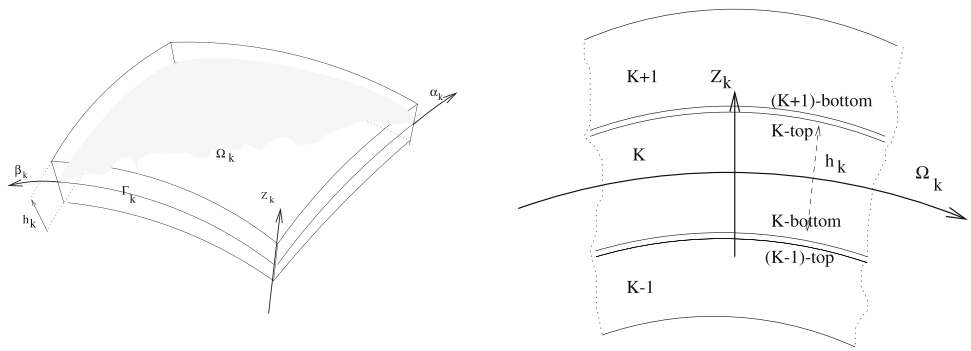

Fig. 3 Geometry and notations for a multilayered shell (*doubly curved*)

static problems we seek the computation of displacements ($\mathbf{u}$) from the global system of equations

$$\mathcal{L}\mathbf{u} = \mathbf{f} \quad \text{in } \Omega \tag{27}$$

$$\mathcal{L}_B\mathbf{u} = \mathbf{g} \quad \text{on } \partial\Omega \tag{28}$$

where $\mathcal{L}$, $\mathcal{L}_B$ are linear operators in the domain and on the boundary, respectively. The right-hand side of (27) and (28) represent the external forces applied on the plate or shell and the boundary conditions applied along the perimeter of the plate or shell, respectively. The PDE problem defined in (27) and (28) will be replaced by a finite problem, defined by an algebraic system of equations, after the radial basis expansions.

3.2 The eigenproblem

The eigenproblem looks for eigenvalues (λ) and eigenvectors ($\mathbf{u}$) that satisfy

$$\mathcal{L}\mathbf{u} + \lambda\mathbf{u} = 0 \quad \text{in } \Omega \tag{29}$$

$$\mathcal{L}_B\mathbf{u} = 0 \quad \text{on } \partial\Omega \tag{30}$$

As in the static problem, the eigenproblem defined in (29) and (30) is replaced by a finite-dimensional eigenvalue problem, based on RBF approximations.

3.3 Radial basis functions approximations

The RBF (ϕ) approximation of a function ($\mathbf{u}$) is given by

$$\widetilde{\mathbf{u}}(\mathbf{x}) = \sum_{i=1}^{N} \alpha_i \phi\left(\|x - y_i\|_2\right), \quad \mathbf{x} \in \mathbb{R}^n \tag{31}$$

where $y_i, i = 1, \ldots, N$ is a finite set of distinct points (centers) in $\mathbb{R}^n$.

The most common RBFs are

Cubic:	$\phi(r) = r^3$
Thin plate splines:	$\phi(r) = r^2 \log(r)$
Wendland functions:	$\phi(r) = (1-r)_+^m p(r)$
Gaussian:	$\phi(r) = e^{-(cr)^2}$
Multiquadrics:	$\phi(r) = \sqrt{c^2 + r^2}$
Inverse Multiquadrics:	$\phi(r) = (c^2 + r^2)^{-1/2}$

where the Euclidian distance r is real and non-negative and c is a positive shape parameter.

Hardy [58] introduced multiquadrics in the analysis of scattered geographical data. In the 1990's Kansa [35] used multiquadrics for the solution of partial differential equations. Considering N distinct interpolations, and knowing $u(x_j)$, $j = 1, 2, \ldots, N$, we find α_i by the solution of a $N \times N$ linear system

$$\mathbf{A}\boldsymbol{\alpha} = \mathbf{u} \tag{32}$$

where $\mathbf{A} = [\phi\left(\|x - y_i\|_2\right)]_{N\times N}$, $\boldsymbol{\alpha} = [\alpha_1, \alpha_2, \ldots, \alpha_N]^T$ and $\mathbf{u} = [u(x_1), u(x_2), \ldots, u(x_N)]^T$.

3.4 Solution of the static problem

The solution of a static problem by RBFs considers N_I nodes in the domain and N_B nodes on the boundary, with a total number of nodes $N = N_I + N_B$. We denote the sampling points by $x_i \in \Omega, i = 1, \ldots, N_I$ and $x_i \in \partial\Omega, i = N_I + 1, \ldots, N$. At the points in the domain we solve the following system of equations

$$\sum_{i=1}^{N} \alpha_i \mathcal{L}\phi\left(\|x - y_i\|_2\right) = \mathbf{f}(x_j), \quad j = 1, 2, \ldots, N_I \tag{33}$$

or

$$\mathcal{L}^I\boldsymbol{\alpha} = \mathbf{F} \tag{34}$$

where

$$\mathcal{L}^I = [\mathcal{L}\phi\left(\|x - y_i\|_2\right)]_{N_I\times N} \tag{35}$$

At the points on the boundary, we impose boundary conditions as

$$\sum_{i=1}^{N} \alpha_i \mathcal{L}_B \phi\left(\|x - y_i\|_2\right) = \mathbf{g}(x_j), \quad j = N_I + 1, \ldots, N \tag{36}$$

or

$$\mathbf{B}\boldsymbol{\alpha} = \mathbf{G} \tag{37}$$

where

$$\mathbf{B} = \mathcal{L}_B \phi\left[\left(\|x_{N_I+1} - y_j\|_2\right)\right]_{N_B \times N}$$

Therefore, we can write a finite-dimensional static problem as

$$\begin{bmatrix} \mathcal{L}^I \\ \mathbf{B} \end{bmatrix} \boldsymbol{\alpha} = \begin{bmatrix} \mathbf{F} \\ \mathbf{G} \end{bmatrix} \tag{38}$$

By inverting the system (38), we obtain the vector $\boldsymbol{\alpha}$. We then obtain the solution $\mathbf{u}$ using the interpolation equation (31).

3.5 Solution of the eigenproblem

We consider N_I nodes in the interior of the domain and N_B nodes on the boundary, with $N = N_I + N_B$. We denote interpolation points by $x_i \in \Omega$, $i = 1, \ldots, N_I$ and $x_i \in \partial\Omega$, $i = N_I + 1, \ldots, N$. At the points in the domain, we define the eigenproblem as

$$\sum_{i=1}^{N} \alpha_i \mathcal{L}\phi\left(\|x - y_i\|_2\right) = \lambda \tilde{\mathbf{u}}(x_j), \quad j = 1, 2, \ldots, N_I \tag{39}$$

or

$$\mathcal{L}^I \boldsymbol{\alpha} = \lambda \tilde{\mathbf{u}}^I \tag{40}$$

where

$$\mathcal{L}^I = \left[\mathcal{L}\phi\left(\|x - y_i\|_2\right)\right]_{N_I \times N} \tag{41}$$

At the points on the boundary, we enforce the boundary conditions as

$$\sum_{i=1}^{N} \alpha_i \mathcal{L}_B \phi\left(\|x - y_i\|_2\right) = 0, \quad j = N_I + 1, \ldots, N \tag{42}$$

or

$$\mathbf{B}\boldsymbol{\alpha} = 0 \tag{43}$$

Equations (40) and (43) can now be solved as a generalized eigenvalue problem

$$\begin{bmatrix} \mathcal{L}^I \\ \mathbf{B} \end{bmatrix} \boldsymbol{\alpha} = \lambda \begin{bmatrix} \mathbf{A}^I \\ \mathbf{0} \end{bmatrix} \boldsymbol{\alpha} \tag{44}$$

where

$$\mathbf{A}^I = \phi\left[\left(\|x_{N_I} - y_j\|_2\right)\right]_{N_I \times N}$$

3.6 Discretization of the equations of motion and boundary conditions

The radial basis collocation method follows a simple implementation procedure. Taking Eq. (13), we compute

$$\boldsymbol{\alpha} = \begin{bmatrix} L^I \\ \mathbf{B} \end{bmatrix}^{-1} \begin{bmatrix} \mathbf{F} \\ \mathbf{G} \end{bmatrix} \tag{45}$$

This $\boldsymbol{\alpha}$ vector is then used to obtain solution $\tilde{\mathbf{u}}$, by using (7). If derivatives of $\tilde{\mathbf{u}}$ are needed, such derivatives are computed as

$$\frac{\partial \tilde{\mathbf{u}}}{\partial x} = \sum_{j=1}^{N} \alpha_j \frac{\partial \phi_j}{\partial x} \tag{46}$$

$$\frac{\partial^2 \tilde{\mathbf{u}}}{\partial x^2} = \sum_{j=1}^{N} \alpha_j \frac{\partial^2 \phi_j}{\partial x^2}, \text{ etc} \tag{47}$$

In the present collocation approach, we need to impose essential and natural boundary conditions. Consider, for example, the condition $w = 0$, on a simply supported or clamped edge. We enforce the conditions by interpolating as

$$w = 0 \rightarrow \sum_{j=1}^{N} \alpha_j^W \phi_j = 0 \tag{48}$$

Other boundary conditions are interpolated in a similar way.

3.7 Free vibrations problems

For free vibration problems we set the external force to zero, and assume harmonic solution in terms of displacements $u_1, u_2, \ldots, v_1, v_2, \ldots,$ as

$$u_1 = U_1(w, y)e^{i\omega t}; \quad u_2 = U_2(w, y)e^{i\omega t};$$
$$u_3 = U_3(w, y)e^{i\omega t}; \quad u_4 = U_4(w, y)e^{i\omega t} \tag{49}$$
$$v_1 = V_1(w, y)e^{i\omega t}; \quad v_2 = V_2(w, y)e^{i\omega t};$$
$$v_3 = V_3(w, y)e^{i\omega t}; \quad v_4 = V_4(w, y)e^{i\omega t} \tag{50}$$
$$w_1 = W_1(w, y)e^{i\omega t}; \quad w_2 = W_2(w, y)e^{i\omega t};$$
$$w_3 = W_3(w, y)e^{i\omega t}; \quad w_4 = W_4(w, y)e^{i\omega t} \tag{51}$$

where ω is the frequency of natural vibration. Substituting the harmonic expansion into Eq. (44) in terms of the amplitudes $U_1, U_2, U_3, U_4, V_1, V_2, V_3, V_4, W_1, W_2, W_3, W_4,$ we may obtain the natural frequencies and vibration modes for the plate or shell problem, by solving the eigenproblem

$$\left[\mathcal{L} - \omega^2 \mathcal{G}\right] \mathbf{X} = \mathbf{0} \tag{52}$$

where $\mathcal{L}$ collects all stiffness terms and $\mathcal{G}$ collects all terms related to the inertial terms. In (52) $\mathbf{X}$ are the modes of vibration associated with the natural frequencies defined as ω.

4 Numerical examples

All numerical examples consider a Chebyshev grid and a Wendland function, defined as

$$\phi(r) = (1 - c\,r)_+^8 \left(32(c\,r)^3 + 25(c\,r)^2 + 8c\,r + 1\right) \quad (53)$$

where the shape parameter (c) was obtained by an optimization procedure, as detailed in Ferreira and Fasshauer [59].

4.1 Spherical shell in bending

A laminated composite spherical shell is here considered, of side a and thickness h, composed of layers oriented at [0°/90°/0°] and [0°/90°/90°/0°]. The shell is subjected to a sinusoidal vertical pressure of the form

$$p_z = P \sin\left(\frac{\pi x}{a}\right) \sin\left(\frac{\pi y}{a}\right)$$

with the origin of the coordinate system located at the lower left corner on the midplane and P the maximum load (at center of shell).

The orthotropic material properties for each layer are given by

$$E_1 = 25.0E_2 \quad G_{12} = G_{13} = 0.5E_2 \quad G_{23} = 0.2E_2 \quad \nu_{12} = 0.25$$

The in-plane displacements, the transverse displacements, the normal stresses and the in-plane and transverse shear stresses are presented in normalized form as

$$\overline{w} = \frac{10^3 w_{(a/2,a/2,0)} h^3 E_2}{Pa^4}, \quad \overline{\sigma}_{xx} = \frac{\sigma_{xx(a/2,a/2,h/2)} h^2}{Pa^2}$$

$$\overline{\sigma}_{yy} = \frac{\sigma_{yy(a/2,a/2,h/4)} h^2}{Pa^2}$$

$$\overline{\tau}_{xz} = \frac{\tau_{xz(0,a/2,0)} h}{Pa}, \quad \overline{\tau}_{xy} = \frac{\tau_{xy(0,0,h/2)} h^2}{Pa^2}$$

The shell is simply-supported on all edges.

In Table 1, an assessment of the present model is presented for the plate case ($R \to \infty$). We compare the deflections obtained with the RBF method with the LW analytical solution given in [29] and the results obtained with two different shell finite elements: MITC4 and MITC9. These elements are based on CUF and they are described in details in [61] and [62], respectively. Various thickness ratios and laminations are considered. In all the cases, the table shows that the present method is in good agreement with the FEM solution.

In Table 2 we compare the static deflections for the present shell model with results of Reddy shell formulation using first-order and third-order shear-deformation theories [60] and the LW analytical solution given in [29]. We consider nodal grids with 13 × 13, 17 × 17, and 21 × 21 points. We consider various values of R/a and two values of a/h (10 and 100). Results are in good agreement for various a/h ratios with the higher-order results of Reddy and the LW analytical solution.

Table 1 Non-dimensional central deflection, $\overline{w} = w\frac{10^2 E_2 h^3}{P_0 a^4}$ for different cross-ply laminated plates

	Method	$a/h = 10$	$a/h = 100$
[0°/90°/0°]	LW [29]	7.4095	4.3400
	Present (13 × 13)	7.2739	4.2924
	Present (17 × 17)	7.2743	4.2941
	Present (21 × 21)	7.2743	4.2943
	MITC4 (13 × 13)	7.2955	4.2573
	MITC4 (17 × 17)	7.3427	4.2915
	MITC4 (21 × 21)	7.3657	4.3082
	MITC9 (5 × 5)	7.4067	4.3375
	MITC9 (9 × 9)	7.4092	4.3397
	MITC9 (13 × 13)	7.4095	4.3399
[0°/90°/90°/0°]	LW [29]	7.3148	4.3420
	Present (13 × 13)	7.1722	4.2871
	Present (17 × 17)	7.1726	4.2887
	Present (21 × 21)	7.1726	4.2889
	MITC4 (13 × 13)	7.2011	4.2593
	MITC4 (17 × 17)	7.2482	4.2935
	MITC4 (21 × 21)	7.2711	4.3102
	MITC9 (5 × 5)	7.3120	4.3396
	MITC9 (9 × 9)	7.3145	4.3418
	MITC9 (13 × 13)	7.3147	4.3420

4.2 Free vibration of spherical and cylindrical laminated shells

We consider nodal grids with 13 × 13, 17 × 17, and 21 × 21 points. In Tables 3 and 4 we compare the nondimensionalized natural frequencies from the present layerwise theory for various cross-ply spherical shells, with analytical solutions by Reddy and Liu [60] who considered both the first-order (FSDT) and the third-order (HSDT) theories. The first-order theory overpredicts the fundamental natural frequencies of symmetric thick shells and symmetric shallow thin shells. The present radial basis function method is compared with analytical results by Reddy [60] and shows excellent agreement.

Table 5 contain nondimensionalized natural frequencies obtained using the the present layerwise theory for cross-ply cylindrical shells with lamination schemes [0/90/0], [0/90/90/0]. Present results are compared with analytical solutions by Reddy and Liu [60] who considered both the

Table 2 Non-dimensional central deflection, $\overline{w} = w\frac{10^2 E_2 h^3}{P_0 a^4}$ variation with various number of grid points per unit length, N for different R/a ratios, for $R_1 = R_2$

	a/h	Method	R/a					
			5	10	20	50	100	10^9
[0°/90°/0°]	10	Present (13 × 13)	6.9514	7.1891	7.2518	7.2700	7.2728	7.2739
	10	Present (17 × 17)	6.9520	7.1895	7.2521	7.2703	7.2731	7.2743
	10	Present (21 × 21)	6.9521	7.1895	7.2522	7.2704	7.2732	7.2743
	10	HSDT [60]	6.7688	7.0325	7.1016	7.1212	7.1240	7.125
	10	FSDT [60]	6.4253	6.6247	6.6756	6.6902	6.6923	6.6939
	10	LW [29]	7.0834	7.3252	7.3883	7.4061	7.4087	7.4095
	100	Present (13 × 13)	1.0300	2.3956	3.5832	4.1606	4.2587	4.2924
	100	Present (17 × 17)	1.0305	2.3966	3.5846	4.1622	4.2603	4.2941
	100	Present (21 × 21)	1.0306	2.3968	3.5848	4.1625	4.2606	4.2943
	100	HSDT [60]	1.0321	2.4099	3.617	4.2071	4.3074	4.3420
	100	FSDT [60]	1.0337	2.4109	3.6150	4.2027	4.3026	4.3370
	100	LW [29]	1.0340	2.4120	3.6172	4.2055	4.3055	4.3400
[0°/90°/90°/0°]	10	Present (13 × 13)	6.8580	7.0902	7.1511	7.1686	7.1712	7.1722
	10	Present (17 × 17)	6.8585	7.0905	7.1514	7.1690	7.1716	7.1726
	10	Present (21 × 21)	6.8586	7.0906	7.1515	7.1690	7.1716	7.1726
	10	HSDT [60]	6.7865	7.0536	7.1237	7.1436	7.1464	7.1474
	10	FSDT [60]	6.3623	6.5595	6.6099	6.6244	6.6264	6.6280
	10	LW [29]	6.9953	7.2322	7.2940	7.3114	7.3139	7.3148
	100	Present (13 × 13)	1.0242	2.3865	3.5753	4.1548	4.2533	4.2871
	100	Present (17 × 17)	1.0247	2.3874	3.5766	4.1563	4.2548	4.2887
	100	Present (21 × 21)	1.0247	2.3876	3.5768	4.1565	4.2551	4.2889
	100	HSDT [60]	1.0264	2.4024	3.6133	4.2071	4.3082	4.3430
	100	FSDT [60]	1.0279	2.4030	3.6104	4.2015	4.3021	4.3368
	100	LW [29]	1.0284	2.4048	3.6142	4.2065	4.3073	4.3420

Table 3 Nondimensionalized fundamental frequencies of cross-ply laminated spherical shells, $\overline{\omega} = \omega\frac{a^2}{h}\sqrt{\rho/E_2}$, laminate ([0°/90°/90°/0°])

a/h	Method	R/a					
		5	10	20	50	100	10^9
10	Present (11 × 11)	11.9560	11.7900	11.7478	11.7360	11.7343	11.7337
	Present (13 × 13)	11.9549	11.7892	11.7472	11.7353	11.7337	11.7331
	Present (17 × 17)	11.9544	11.7889	11.7469	11.7351	11.7334	11.7329
	Present (19 × 19)	11.9544	11.7889	11.7469	11.7351	11.7334	11.7328
	HSDT [60]	12.040	11.840	11.790	11.780	11.780	11.780
100	Present (11 × 11)	31.1653	20.4712	16.7365	15.5286	15.3482	15.2876
	Present (13 × 13)	31.1374	20.4524	16.7208	15.5138	15.3336	15.2730
	Present (17 × 17)	31.1275	20.4460	16.7157	15.5092	15.3290	15.2684
	Present (19 × 19)	31.1265	20.4455	16.7153	15.5088	15.3287	15.2681
	HSDT [60]	31.100	20.380	16.630	15.420	15.230	15.170

first-order (FSDT) and the third-order (HSDT) theories. The present radial basis funtion method is compared with analytical results by Reddy [60] and shows excellent agreement.

In Fig. 4 we illustrate the first four vibrational modes of cross-ply laminated spherical shells, $\overline{\omega} = \omega\frac{a^2}{h}\sqrt{\rho/E_2}$, for a laminate ([0°/90°/90°/0°]), using a grid of 13 × 13 points,

Table 4 Nondimensionalized fundamental frequencies of cross-ply laminated spherical shells, $\overline{\omega} = \omega \frac{a^2}{h} \sqrt{\rho / E_2}$, laminate ([0°/90°/0°])

a/h	Method	R/a					
		5	10	20	50	100	10^9
10	Present (11 × 11)	11.8748	11.7803	11.6660	11.6542	11.6524	11.6519
	Present (13 × 13)	11.8736	11.7075	11.6654	11.6535	11.6518	11.6513
	Present (17 × 17)	11.8732	11.7073	11.6652	11.6533	11.6516	11.6511
	Present (19 × 19)	11.8732	11.7072	11.6651	11.6533	11.6516	11.6510
	HSDT [60]	12.060	11.860	11.810	11.790	11.790	11.790
100	Present (11 × 11)	31.0775	20.4310	16.7165	15.5158	15.4993	15.4398
	Present (13 × 13)	31.0501	20.4133	16.7023	15.5028	15.4948	15.4353
	Present (17 × 17)	31.0402	20.4070	16.6973	15.4982	15.4944	15.4349
	Present (19 × 19)	31.0402	20.4065	16.6969	15.6714	15.4944	15.4349
	HSDT [60]	31.0398	20.350	16.620	15.420	15.240	15.170

Table 5 Nondimensionalized fundamental frequencies of cross-ply cylindrical shells, $\overline{\omega} = \omega \frac{a^2}{h} \sqrt{\rho / E_2}$

R/a	Method	[0/90/0]		[0/90/90/0]	
		$a/h = 100$	$a/h = 10$	$a/h = 100$	$a/h = 10$
5	Present (13 × 13)	20.3671	11.8736	20.4082	11.7527
	Present (17 × 17)	20.3554	11.8732	20.3985	11.7523
	Present (19 × 19)	20.3544	11.8732	20.3976	11.7523
	FSDT [60]	20.332	12.207	20.361	12.267
	HSDT [60]	20.330	11.850	20.360	11.830
10	Present (13 × 13)	16.6903	11.7075	16.7093	11.7380
	Present (17 × 17)	16.6836	11.7073	16.7032	11.7377
	Present (19 × 19)	16.6831	11.7073	16.7027	11.7377
	FSDT [60]	16.625	12.173	16.634	12.236
	HSDT [60]	16.620	11.800	16.630	11.790
100	Present (13 × 13)	15.2784	11.6518	15.2880	11.7331
	Present (17 × 17)	15.2739	11.6516	15.2835	11.7329
	Present (19 × 19)	15.2736	11.6516	15.2832	11.7329
	FSDT [60]	15.198	12.163	15.199	12.227
	HSDT [60]	15.19	11.79	15.19	11.78
Plate	Present (13 × 13)	15.2635	11.6513	15.2730	11.7331
	Present (17 × 17)	15.2590	11.6511	15.2684	11.7329
	Present (19 × 19)	15.2587	11.6511	15.2681	11.7329
	FSDT [60]	15.183	12.162	15.184	12.226
	HSDT [60]	15.170	11.790	15.170	11.780

for $a/h = 100$, $R/a = 10$. The modes of vibration are quite stable.

5 Concluding remarks

In this paper a layerwise shear deformation theory was implemented for the first time for laminated orthotropic elastic shells through a multiquadrics discretization of equations of motion and boundary conditions. The multiquadric RBF method for the solution of shell bending and free vibration problems was presented. Results for static deformations and natural frequencies were obtained and compared with other sources. This meshless approach demonstrated that is very successful in the static deformations and free vibration analysis of laminated composite shells. Advantages of RBFs are

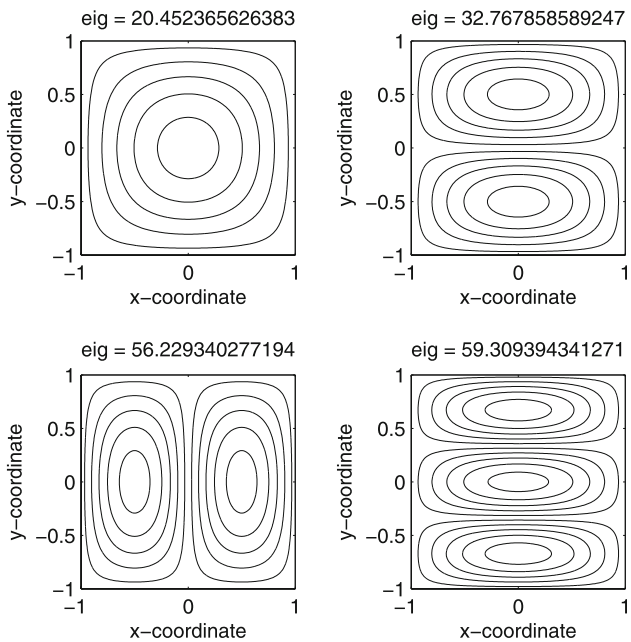

Fig. 4 First four vibrational modes of cross-ply laminated spherical shells, $\overline{\omega} = \omega \frac{a^2}{h} \sqrt{\rho / E_2}$, laminate ([0°/90°/90°/0°]) grid 13 × 13 points, $a/h = 100$, $R/a = 10$

absence of mesh, ease of discretization of boundary conditions and equations of equilibrium or motion and very easy coding. We show that the static displacements and stresses and the natural frequencies obtained from present method are in excellent agreement with analytical solutions.

References

1. Koiter WT (1970) On the foundations of the linear theory of thin elastic shell. Proc Kon Nederl Akad Wetensch 73:169–195
2. Naghdi PM (1956) A survey of recent progress in the theory of elastic shells. Appl Mech Rev 9:365–368
3. Ren JG (1987) Exact solutions for laminated cylindrical shells in cylindrical bending. Compos Sci Technol 29:169–187
4. Varadan TK, Bhaskar K (1991) Bending of laminated orthotropic cylindrical shells—an elasticity approach. Compos Struct 17:141–156
5. Noor AK, Rarig PL (1974) Three-dimensional solutions of laminated cylinders. Comput Methods Appl Mech Eng 3:319–334
6. Noor AK, Peters WS (1989) Stress, vibration and buckling of multilayered cylinders. J Struct Eng ASCE 115:69–89
7. Noor AK, Peters WS (1989) A posteriori estimates for shear correction factors in multilayered composite cylinders. J Eng Mech ASCE 115:1225–1245
8. Ye JQ, Soldatos KP (1994) Three-dimensional vibration of laminated cylinders and cylindrical panels with symmetric or antisymmetric cross-ply lay-up. Compos Eng 4:429–444
9. Grigolyuk EI, Kulikov GM (1988) General direction of the development of the theory of shells. Mekhanica Kompozitnykh Materialov 2:287–298
10. Kapania RK, Raciti S (1989) Recent advances in analysis of laminated beams and plates. AIAA J 27:923–946
11. Kapania RK (1989) A review on the analysis of laminated shells. J Press Vessel Technol 111:88–96
12. Noor AK, Burton WS (1989) Assessment of shear deformation theories for multilayered composite plates. Appl Mech Rev 41:1–18
13. Noor AK, Burton WS (1990) Assessment of computational models for multilayered composite shells. Appl Mech Rev 43:67–97
14. Noor AK, Burton WS, Bert CW (1996) Computational model for sandwich panels and shells. Appl Mech Rev 49:155–199
15. Soldatos KP, Timarci T (1993) A unified formulation of laminated composites, shear deformable, five-degrees-of-freedom cylindrical shell theories. Compos Struct 25:165–171
16. Reddy JN (1997) Mechanics of laminated composite plates, theory and analysis. CRC Press, Boca Raton
17. Hsu T, Wang JT (1970) A theory of laminated cylindrical shells consisting of layers of orthotropic laminae. AIAA J 8:2141–2146
18. Cheung YK, Wu CI (1972) Free vibrations of thick, layered cylinders having finite length with various boundary conditions. J Sound Vib 24:189–200
19. Srinivas S (1973) A refined analysis of composite laminates. J Sound Vib 30:495–550
20. Sun CT, Whitney JM (1973) On the theories for the dynamic response of laminated plates. AIAA J 11:372–398
21. Barbero EJ, Reddy JN, Teply JL (1990) General two-dimensional theory of laminated cylindrical shells. AIAA J 28:544–553
22. Cho KN, Bert CW, Striz AG (1991) Free vibrations of laminated rectangular plates analyzed by higher order individual-layer theory. J Sound Vib 145:429–442
23. Nosier A, Kapania RK, Reddy JN (1993) Free vibration analysis of laminated plates using a layer-wise theory. AIAA J 31:2335–2346
24. Gaudenzi P, Barboni R, Mannini A (1995) A finite element evaluation of single-layer and multi-layer theories for the analysis of laminated plates. Compos Struct 30:427–440
25. Carrera E (1998) Evaluation of layer-wise mixed theories for laminated plates analysis. AIAA J 36:830–839
26. Carrera E (1998) Layer-wise mixed models for accurate vibration analysis of multilayered plates. J Appl Mech 65:820–828
27. Carrera E (2003) Theories and finite elements for multilayered plates and shells: a unified compact formulation with numerical assessment and benchmarking. Arch Comput Methods Eng 97:10–215
28. Carrera E (1999) Multilayered shell theories accounting for layerwise mixed description. Part 1: governing equations. AIAA J 37(9):1107–1116
29. Carrera E (1999) Multilayered shell theories accounting for layerwise mixed description. Part 2: numerical evaluations. AIAA J 37(9):1117–1124
30. Carrera E (1999) A study of transverse normal stress effect on vibration of multilayered plates and shells. J Sound Vib 225(5):803–829
31. Carrera E (1998) A Reissner's mixed variational theorem applied to vibrational analysis of multilayered shell. J Appl Mech 66:63–78
32. Dennis ST, Palazotto AN (1989) Transverse shear deformation in orthotropic cylindrical pressure vessels using a higher-order shear theory. AIAA J 27(10):1441–1447
33. Merk J (1995) Hierarchische, Kontinuumbasiert Shalenelemente höhere Ordnung. PhD Dissertation, Institute for Statics and Dynamics, Universität Stuttgart, Stuttgart, Germany
34. Di S, Ramm E (1993) Hybrid stress formulation for higher-order theory of laminated shell analysis. Comput Method Appl Mech Eng 109:359–376
35. Kansa EJ (1990) Multiquadrics: a scattered data approximation scheme with applications to computational fluid dynamics. I: Surface approximations and partial derivative estimates. Comput Math Appl 19(8/9):127–145

36. Hon YC, Lu MW, Xue WM, Zhu YM (1997) Multiquadric method for the numerical solution of byphasic mixture model. Appl Math Comput 88:153–175
37. Hon YC, Cheung KF, Mao XZ, Kansa EJ (1999) A multiquadric solution for the shallow water equation. ASCE J Hydraul Eng 125(5):524–533
38. Wang JG, Liu GR, Lin P (2002) Numerical analysis of biot's consolidation process by radial point interpolation method. Int J Solids Struct 39(6):1557–1573
39. Liu GR, Gu YT (2001) A local radial point interpolation method (LRPIM) for free vibration analyses of 2-d solids. J Sound Vib 246(1):29–46
40. Liu GR, Wang JG (2002) A point interpolation meshless method based on radial basis functions. Int J Numer Methods Eng 54:1623–1648
41. Wang JG, Liu GR (2002) On the optimal shape parameters of radial basis functions used for 2-d meshless methods. Comput Methods Appl Mech Eng 191:2611–2630
42. Chen XL, Liu GR, Lim SP (2003) An element free galerkin method for the free vibration analysis of composite laminates of complicated shape. Compos Struct 59:279–289
43. Dai KY, Liu GR, Lim SP, Chen XL (2004) An element free galerkin method for static and free vibration analysis of shear-deformable laminated composite plates. J Sound Vib 269:633–652
44. Liu GR, Chen XL (2002) Buckling of symmetrically laminated composite plates using the element-free galerkin method. Int J Struct Stab Dyn 2:281–294
45. Liew KM, Chen XL, Reddy JN (2004) Mesh-free radial basis function method for buckling analysis of non-uniformity loaded arbitrarily shaped shear deformable plates. Comput Methods Appl Mech Eng 193:205–225
46. Huang YQ, Li QS (2004) Bending and buckling analysis of anti-symmetric laminates using the moving least square differential quadrature method. Comput Methods Appl Mech Eng 193:3471–3492
47. Liu L, Liu GR, Tan VCB (2002) Element free method for static and free vibration analysis of spatial thin shell structures. Comput Methods Appl Mech Eng 191:5923–5942
48. Xiang S, Wang KM, Ai YT, Sha YD, Shi H (2009) Analysis of isotropic, sandwich and laminated plates by a meshless method and various shear deformation theories. Compos Struct 91(1):31–37
49. Xiang S, Shi H, Wang KM, Ai YT, Sha YD (2010) Thin plate spline radial basis functions for vibration analysis of clamped laminated composite plates. Eur J Mech A Solids 29:844–850
50. Ferreira AJM, Roque CMC, Jorge RMN (2006) Analysis of composite and sandwich plate by trigonometric layer-wise deformation theory and radial basis function. J Sandwich Struct Mater 8:497–515
51. Ferreira AJM (2003) A formulation of the multiquadric radial basis function method for the analysis of laminated composite plates. Compos Struct 59:385–392
52. Ferreira AJM (2003) Thick composite beam analysis using a global meshless approximation based on radial basis functions. Mech Adv Mater Struct 10:271–284
53. Ferreira AJM, Roque CMC, Martins PALS (2003) Analysis of composite plates using higher-order shear deformation theory and a finite point formulation based on the multiquadric radial basis function method. Compos B 34:627–636
54. Carrera E (2001) Developments, ideas, and evaluations based upon reissner's mixed variational theorem in the modelling of multilayered plates and shells. Appl Mech Rev 54:301–329
55. Carrera E (1996) C^0 Reissner-Mindlin multilayered plate elements including zig-zag and interlaminar stress continuity. Int J Numer Methods Eng 39:1797–1820
56. Carrera E, Kroplin B (1997) Zig-zag and interlaminar equilibria effects in large deflection and post-buckling analysis of multilayered plates. Mech Compos Mater Struct 4:69–94
57. Carrera E (1998) Evaluation of layer-wise mixed theories for laminated plate analysis. AIAA J 36:830–839
58. Hardy RL (1971) Multiquadric equations of topography and other irregular surfaces. Geophys Res 176:1905–1915
59. Ferreira AJM, Fasshauer GE (2006) Computation of natural frequencies of shear deformable beams and plates by a rbf-pseudospectral method. Comput Methods Appl Mech Eng 196:134–146
60. Reddy JN, Liu CF (1985) A higher-order shear deformation theory of laminated elastic shells. Int J Eng Sci 23:319–330
61. Cinefra M, Carrera E, Nali P (2010) MITC technique extended to variable kinematic multilayered plate elements. Compos Struct 92:1888–1895
62. Cinefra M, Chinosi C, Della Croce L (2011) MITC9 shell elements based on refined theories for the analysis of isotropic cylindrical structures. Mech Adv Mater Struct (in press)